Biosensors and Bioelectronics 141 (2019) 111471

Contents lists available at ScienceDirect

Biosensors and Bioelectronics

journal homepage: www.elsevier.com/locate/bios

Wearable high-powered biofuel cells using enzyme/carbon nanotube composite fibers on textile cloth

Sijie Yin, Zewen Jin, Takeo Miyake*

Graduate School of Information Production and Systems, Waseda University, 2-7 Hibikino Wakamatsuku Kitakyushushi, Fukuoka, Japan

ARTICLE INFO

Keywords:
Wearable power source
Biofuel cell
Series-connection
Bioelectrode
Enzyme-nanotube hybrid

ABSTRACT

Wearable biofuel cells with flexible enzyme/carbon nanotube (CNT) fibers were designed on a cotton textile cloth by integrating two components: bioanode fibers for glucose oxidation and O_2-diffusion biocathode fibers for oxygen reduction. The anode and cathode fibers were prepared through modification with glucose dehydrogenase and bilirubin oxidase, respectively, on multi-walled carbon nanotube-coated carbon fibers. Both biofibers woven on the cloth generated a power density of 48 μW/cm^2 at 0.24 V from 0.1 mM glucose (human sweat amount), and of 216 μW/cm^2 at 0.36 V, when glucose was supplied from a hydrogel tank containing 200 mM glucose. Our fiber-based biofuel cell deformed to an S-shape without a significant loss in cell performance. Furthermore, we demonstrated a series-connection involving the tying of biofibers on a cloth with batik-based ionic isolation. The booster four cells generate power at 1.9 V that illuminated an LED on the cloth.

1. Introduction

There is increasing interest for the development of wearable electronic devices, including functional artificial electric skin (Hammock et al., 2013; Sun et al., 2018), wearable displays (Park et al., 2009; Sekitani et al., 2009), and health monitoring devices (Hattori et al., 2014; Oh et al., 2018; Yamada et al., 2011). The production of such electronic devices requires all components, including the power source to be flexible and stretchable so that the devices can be transformed to twisted, stretched, and folded forms. Conventional chemical batteries are unsuitable for wearable electronics due to rigidity and toxicity. Therefore, safe and comfortable power sources are required for wearable electronics.

Enzyme-based biofuel cells (BFCs) are prospective candidates for wearable and sustainable power sources (Minteer et al., 2007; Willner et al., 2009) because power generation originates from the carbohydrate biofuels produced by living systems (Akers et al., 2005; Ramanavicius et al., 2005). Examples include power generation from blood (Southcott et al., 2013), sweat (Bandodkar et al., 2017; Jeerapan et al., 2016; Jia et al., 2013; Lv et al., 2018), tears (Falk et al., 2012), and urine (Göbel et al., 2016). The strategy to develop BFCs involves using new functional carbon-rich micro/nano-materials for enzyme loading due to their large specific surface area. Ketjenblack (Miyake et al., 2009) and carbon black (Tamaki et al., 2007) coated microelectrodes are commonly used to enhance enzymatic BFC performance. Carbon electrodes with MgO template provide a large surface area with precise control of the pore sizes for enzyme loading and sufficient biofuel supply (Murata et al., 2014; Shitanda et al., 2015). The carbon nanotube (CNT) is a cutting-edge material that provides high conductivity, mechanical strength, and surface functionalization. Recently, CNT-based films (Bandodkar et al., 2015; Miyake et al., 2011b), fibers (Li et al., 2008; Sim et al., 2018), and yarn (Kwon et al., 2014) were produced to enhance the output current (from the μA to the mA) from artificial biofluids. However, the current from natural products such as sweat and tears still remains at the μA level due to insufficient supply of biofuel to nanostructured carbon electrodes. Furthermore, the wearable cell voltage is around 1.0 V when powered from a BFC, and this output voltage is insufficient to operate devices for some applications. The output voltage can be boosted using the following: (1) a DC/DC boost converter, or (2) a series connection of multiple BFCs on the textile cloth. For examples, a single BFC was connected with a charge pump IC-based circuit to boost the cell voltage from 0.6 to 2.0 V (Katz and MacVittie, 2013). This circuit assisted in providing LED illumination from grape (Miyake et al., 2011a) and snail (Katz, 2015), and for a wireless biosensing system (Hanashi et al., 2011; Kassal et al., 2015). In contrast, the use of a series connection of multiple BFCs produces a net output voltage over 1.0 V. Examples include microfluidic BFCs with superhydrophobic air valves (Togo et al., 2009); layered BFCs sequentially laminating bioanode carbon sheets, a hydrogel tank, including biofuels, and biocathode carbon sheets (Miyake et al., 2013); and

* Corresponding author.
E-mail address: miyake@waseda.jp (T. Miyake).

https://doi.org/10.1016/j.bios.2019.111471
Received 4 April 2019; Received in revised form 18 June 2019; Accepted 22 June 2019
Available online 24 June 2019
0956-5663/

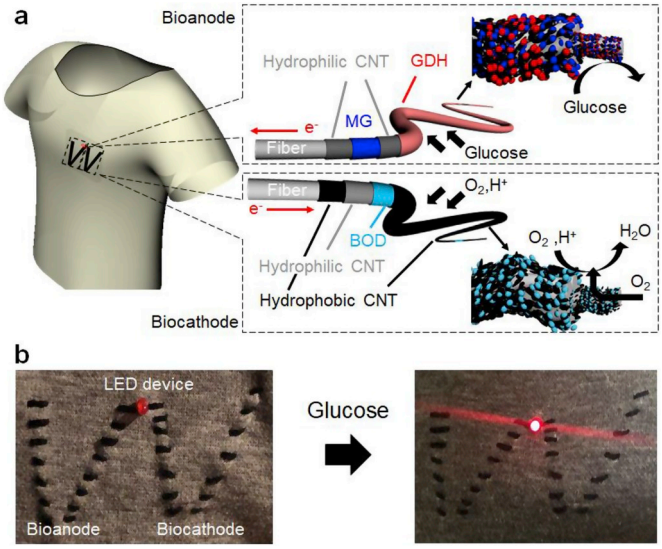

Fig. 1. a. Schematic of enzyme/CNT composite fibers woven on a textile cloth. b. Illumination of an LED device (charge pump IC, capacitor and red LED) connected to enzymatic power fibers when a glucose solution is dropped on a cloth. (For interpretation of the references to colour in this figure legend, the reader is referred to the Web version of this article.)

screen-printed origami BFCs (Shitanda et al., 2017). Efforts, however, were devoted on producing enzymatic cells on solid substrates or on carbon fabric strips. Although mounting on planar surfaces of a textile cloth for wearable skin devices is possible for such two-dimensional BFCs, application on curvy surfaces like the eye lens, the ankle and the elbow remains difficult. To this end, one-dimensional fiber BFCs are suitable for designing 2D or 3D cells of complex curvatures by weaving the enzyme fibers.

Here, we develop flexible enzyme/CNT composite fibers for power generation on a textile cloth using glucose biofuel (Fig. 1) and demonstrate a series connection by tying the enzyme fibers with batik-based ionic isolation to boost the net output voltage and power. The anode and cathode fibers were prepared by modifying multi-walled CNT (MWCNT)-decorated carbon fibers with glucose dehydrogenase (GDH) and bilirubin oxidase (BOD), respectively. We optimized the performance in a nicotinamide adenine dinucleotide (NAD)-cofactor GDH bioanode with hydrophilic CNT coating, and in an O_2-diffusion biocathode with multi-coating of the hydrophobic and hydrophilic CNTs on the fibers. The flexible fiber-based BFC yields high power even when deformed to an S shape at temperatures from 4 to 50 °C. Furthermore, we demonstrate illumination of an LED device powered by a BFC and boosted by four BFCs on the textile cloth with a glucose solution input.

2. Material and methods

2.1. Reagents

The MWCNTs used were purchased from Cheap Tubes (> 95% purity, 30–50 nm diameter, 10–20 μm length, functionalized COOH group). Methylene green (MG) was purchased from MP Biomedicals, and NAD^+ was obtained from Oriental Yeast Co. GDH (30 U/mg), D (+)-Glucose, Triton X-100, ethanol (99.5), HNO_3, H_2SO_4, K_2HPO_4, and KH_2PO_4 were purchased from FUJIFILM Wako. The BOD was purchased from Amano Enzyme Inc, and the carbon fiber was bought from FC-R&D (0.1 mm diameter). Textile cloth was purchased from UNIQLO. Polytetrafluoroethylene (PTFE) was purchase from SIGMA-ALDRICH.

2.2. Acid-treatment for CNT

The MWCNT was heated at 400 °C for 11 h in an oven. This was followed by treatment with a mixed acid solution (distilled water: HNO_3: H_2SO_4 with a volume ratio of 1:3:1) for 30 min in an ultrasonic bath at 4 °C and, subsequently, in a static bath for 5 h at room temperature. After neutralizing the acid with NaOH solution, acid-treated CNT (A-CNT) was dispersed in a solution, collected by vacuum filtration, and freeze-dried to prevent aggregation of the CNTs during drying.

2.3. Preparation of carbon fiber anode

A 500 μL aliquot of 5 mg/mL A-CNT solution containing 1% Triton X-100 was dropped onto carbon fibers and dried in an oven at 70 °C, followed by washing of the A-CNT modified carbon fibers with distilled water to remove excess A-CNT. The A-CNT carbon fibers were decorated with a PolyMG mediator for NADH oxidation at a cyclic voltage between −0.4 and 0.6 V vs. Ag/AgCl for five cycles to the fibers in the PBS buffer (0.1 M, pH 7) including 2 mM MG. After washing with water, we adsorbed GDH enzymes onto PolyMG/A-CNT carbon fibers in a stirring solution, containing 0.4 mg/mL GDH at 4 °C for 24 h to produce a composite that we refer to as GDH/PolyMG/A-CNT/fibers. In addition, before loading the GDH enzymes into the CNT fibers, we coated the A-CNT on the PolyMG/A-CNT carbon fibers and allowed subsequent GDH enzyme adsorption on the electrode to produce GDH/A-CNT/PolyMG/A-CNT/fibers. A geometric area of 0.12 cm^2 was utilized for the calculation of the current density in cyclic voltammetry.

2.4. Preparation of O_2-diffusion cathode

In the cathode preparation, we used two types of CNT solutions including a 5 mg/mL hydrophilic A-CNT solution containing 1% Triton X-100 for BOD enzyme loading and proton flow, and a 5-mg/mL hydrophobic MWCNT ethanol solution with 1.0 wt% PTFE hydrophobic particles to produce a PTFE-CNT layer for O_2 diffusion from air. As in the anode preparation, we coated A-CNT on carbon fibers, allowed adsorption of the BOD enzyme onto the A-CNT/fibers in a stirred solution containing 5 mg/mL BOD at 4 °C for 12 h and termed it BOD/A-CNT/fiber. We coated further PTFE-CNT layer onto the BOD/A-CNT/fiber (PTFE-CNT/BOD/A-CNT/fiber) by drop-casting at room temperature. Two additional BOD cathodes were prepared by coating the carbon fibers BOD/A-CNT/PTFE-CNT/fiber and PTFE-CNT/BOD/A-CNT/PTFE-CNT/fiber with PTFE-CNT. The current density was calculated using a geometric area of 0.12 cm^2.

2.5. Preparation of hydrogel sheet

The preparation of the hydrogel sheet followed the procedures used by Ogawa et al., (2015). The polyacrylamide prepolymer solution was composed of 5 wt% acrylamide, 0.24 wt% N,N-methylene-bis-acrylamide, and 1 mg/mL Irgacure 2959 (BASF Japan Ltd.). The prepolymer solution was poured into a 50 mm × 100 mm × 5 mm (w × l × h) silicone-rubber chamber on a glass substrate and then UV-irradiated (LC8, HAMAMATSU) until polymerized. Each hydrogel sheet was immersed overnight in 0.1 mM PBS buffer (pH 7.0), including 10 mM NAD^+ and glucose varying from 0 to 200 mM. The ionic conductivity of the prepared hydrogel measured by AC impedance spectroscopy (± 5 mV, 1–10,000 Hz) was 2 Ω.

2.6. Electrochemical measurements

The performance of the carbon fiber electrodes was analyzed by a three-electrode system (BAS, 2325 model or Hokuto Denko, HSV-110 electrochemical analyzer) in solution using an Ag/AgCl reference and a platinum counter electrode. The GDH-modified anodes were evaluated in a glucose solution, whereas the BOD-modified cathodes were

evaluated in a PBS solution. The performance of the biofuel cell was evaluated based on the cell voltage upon connecting with a variable external resistance between 0.9 and 80 kΩ before and after sewing enzyme fibers on the cloth. The current and the power were derived from the cell voltage and the resistance. The electrochemical measurements were carried out at different temperatures: at 4 °C in a refrigerator and at 20, 30, and 50 °C in an oven.

2.7. Preparation of batik-based ionic isolation

Beeswax (Dharma Trading Co., melting point: 62 °C) was used as a hydrophobic flame on the textile cloth. To melt the max, we heated it with a gas burner, and the melted max was dropped on both sides of the cloth to create four square flames. This was followed by placing the max flamed cloth on a hot plate at 80 °C for 5 min to create seamless and smooth flames.

3. Results and discussion

3.1. Performance of GDH-CNT composite bioanodes

The GDH enzyme catalyzes the oxidation of glucose by reducing the co-factor NAD^+ to NADH so that NADH oxidation at the anodic electrode sustains the continuous oxidation reaction. However, NADH oxidation at conventional electrodes requires a large overvoltage of 0.35 V for gold (Neto et al., 2015) and 0.8 V for glassy carbon electrodes (Pillai et al., 2018). Thus, a common strategy for reducing this overvoltage involves adding a mediator (Bilgi et al., 2018) and/or the diaphorase enzyme (Dinh et al., 2016) on the electrodes. Here, we used PolyMG as a mediator due to its excellent electrocatalytic activity and stability toward NADH oxidation (Carucci et al., 2017). First, we investigated NADH oxidation at the electropolymerized MG on the A-CNT/fiber. The results show that the oxidation current starts at a negative potential of −0.2 V, and the maximum current density of 15 mA/cm^2 is reached at 0.2 V for a 10 mM NADH solution (Supporting Fig. 1). In the absence of NADH in a PBS solution, we observed only small redox peaks from the adsorbed PolyMG mediator on the fiber electrode.

To perform the glucose oxidation, we modified the GDH on the PolyMG/A-CNT/fiber electrode (Fig. 2a). The oxidation current density was 1.8 mA/cm^2 at 0.17 V in the presence of 10 mM NAD^+ and 200 mM glucose at 50 °C. This value was obviously small as compared with pre-measurements of NADH oxidation at the PolyMG/A-CNT/fiber electrode (Supporting Fig. 1). We assume that the electropolymerized MG blocked the GDH loading onto the A-CNT fiber. In fact, when we measured the glucose oxidation at the GDH/A-CNT/fiber without the PolyMG mediator (Fig. 2a), the current density was 6.4 mA/cm^2 at the same condition, whereas this mediator-less electrode required an overvoltage of 0.42 V. To resolve this issue, we added a layer of A-CNT for GDH loading onto the PolyMG/A-CNT/fiber electrode. The performance was enhanced dramatically to 7.6 mA/cm^2 at 0.16 V, which is 4.2 times that obtained with the GDH/PolyMG/A-CNT/fiber. We optimized the amount of additional A-CNT coating (Supporting Fig. 2) and found that the performance increased to five times the coating due to large GDH biocatalysts. The five times increase in the A-CNT coating maintain the performance.

To calibrate the performance of our GDH-based fiber at different temperatures, we measured the oxidation current at 4 °C, 20 °C, 30 °C, and 50 °C (Fig. 2b). Understanding the temperature dependency is important because of the environmental temperature difference between locations as well as between the inside and outside of buildings. We assumed that a wearable cell functions on the body due to the temperature gradient between the body temperature (around 36 °C) and the ambient environmental temperature. The oxidation current using the GDH/A-CNT/PolyMG/A-CNT/fiber electrode at 0.16 V was 1.4 mA/cm^2 at 4 °C, 4.9 mA/cm^2 at 20 °C, 5.7 mA/cm^2 at 30 °C, and 7.6 mA/cm^2 at 50 °C. Increasing the temperature of the solution enhanced the performance because the GDH activity depends on temperature. The optimum temperature for the GDH activity was 50 °C (Yasuhira et al., 2010), and therefore, further decrease in the oxidation current was possible by raising the temperature to 60 °C.

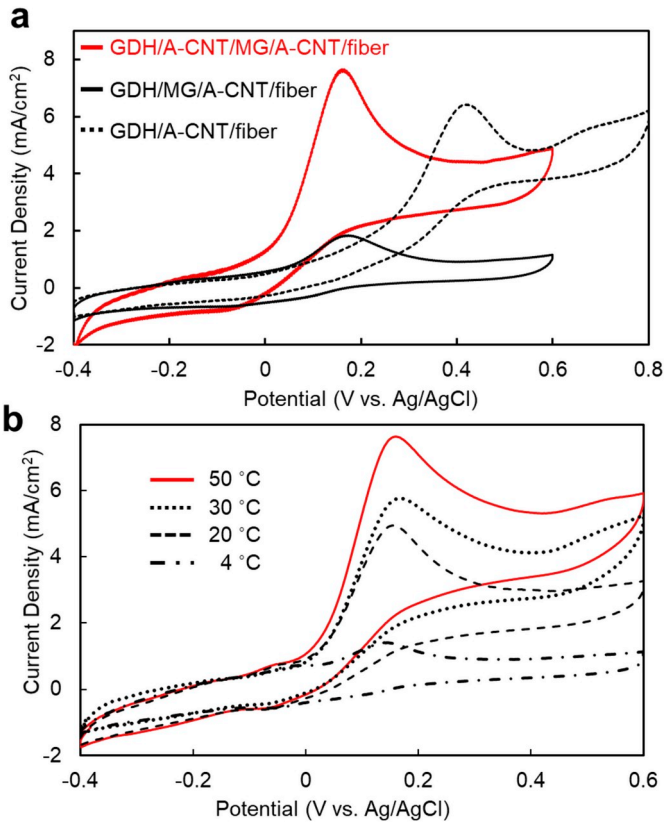

Fig. 2. a. Cyclic voltammograms of glucose oxidation at 20 mV s^{-1} in a 100 mM buffer solution (pH 7) containing 200 mM glucose and 10 mM NAD^+. The PolyMG/A-CNT/fiber electrodes were modified using 0.4 mg/mL GDH (black line) or using both 5 mg/mL A-CNT and 0.4 mg/ml GDH (red line). The data from the mediator-less electrode (GDH/A-CNT/fiber, broken black line) was added. b. Current density using GDH/A-CNT/PolyMG/A-CNT/fiber at different temperatures when we applied the cyclic potential vs. Ag/AgCl. (For interpretation of the references to colour in this figure legend, the reader is referred to the Web version of this article.)

3.2. Performance of the BOD-CNT composite biocathode

The BOD enzyme catalyzes the reduction of oxygen to water according to $O_2 + 4H^+ + 4e^- \rightarrow 2H_2O$ and receives an electron directly from the supporting electrode (Nishizawa, 2019). In general, the low solubility and small diffusion coefficient of dissolved oxygen in aqueous solutions (Weissenborn and Pugh, 1996) cause the performance of BOD-based electrodes to be measured in stirring solutions (Ikeda, 2012), but such electrodes are incompatible for practical use. Instead, engineering a gas-diffusion electrode allows performing the BOD reaction by supplying oxygen from ambient air. Although efforts to produce a BOD-based gas-diffusion electrode on a planer substrate are well-known, there are no reports on a gas-diffusion fiber production from enzyme catalysts.

As in the case of the anodic electrode, we coated the BOD on the A-CNT/fiber electrode (BOD-fiber 1) and measured the performance of the 40-mm–long BOD-fiber 1 with the three-electrode system in a static PBS solution (Fig. 3a). During the measurement, we exposed most of the BOD-fiber to a solution (35 mm length in the solution and 5 mm length in air). The current density of 0.1 mA/cm^2 at 0 V changed to 2 mA/cm^2 under stirring and oxygen-rich conditions. To improve the oxygen

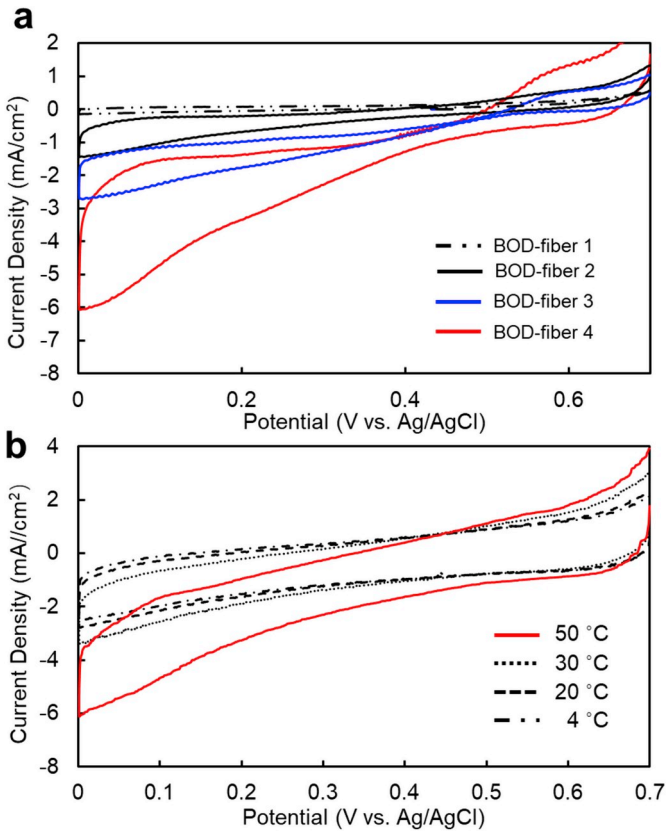

Fig. 3. a. Cyclic voltammograms of oxygen reduction at 20 mV s^{-1} in a 100 mM buffer solution (pH 7). The A-CNT/fiber electrode was modified with 5 mg/mL BOD (broken black line, BOD/A-CNT/fiber, BOD-fiber 1). A hydrophobic layer of PTFE-CNT was added on bare fiber (black line, BOD/A-CNT/PTFE-CNT/fiber, BOD-fiber 2) or on the BOD/A-CNT/fiber electrode (blue line, PTFE-CNT/BOD/A-CNT/fiber, BOD-fiber 3). Furthermore, we designed the sandwich structure of the GDH/A-CNT layer between the PTFE-CNT layers (red line, PTFE-CNT/BOD/A-CNT/PTFE-CNT/fiber, BOD-fiber 4). b. Current density using BOD-fiber 4 at different temperatures when we applied the cyclic potential vs. Ag/AgCl. (For interpretation of the references to colour in this figure legend, the reader is referred to the Web version of this article.)

supply to the electrode, we added a hydrophobic layer of PTFE-CNT on the bare fiber (BOD/A-CNT/PTFE-CNT/fiber, BOD-fiber 2) or on the BOD/A-CNT/fiber electrode (PTFE-CNT/BOD/A-CNT/fiber, BOD-fiber 3). The performance was enhanced to 1.2 mA/cm^2 using BOD-fiber 2 and to 2.7 mA/cm^2 using BOD-fiber 3, compared to that using BOD-fiber 1. In the BOD-fiber 2 structure, the internal hydrophobic PTFE-CNT and the outer hydrophilic BOD/A-CNT layers supply the oxygen from the air and the proton from the solution, respectively. In contrast, the outer PTFE-CNT and the internal BOD/A-CNT layers in the BOD-fiber 3 structure supply the oxygen and the proton, respectively. Moreover, placing a hydrophilic proton transporting BOD/A-CNT layer between consecutive hydrophobic gas-diffusing PTFE-CNT layers to support the carbon fiber (PTFE-CNT/BOD/A-CNT/PTFE-CNT/fiber, BOD-fiber 4) enhanced its performance by 60 to 6 mA/cm^2 at 0 V, relative to that using BOD-fiber 1. This is because the multilayered structure provided efficient proton transfer through the hydrophilic A-CNT layer and oxygen diffusion from the air through the hydrophobic PTFE-CNT double layers to the BOD catalysts in contact with the fiber electrode. We also measured the performance of BOD-fiber4 at 4 °C, 20 °C, 30 °C, and 50 °C. The current density at 0 V was 2.5 mA/cm^2 at 4 °C, 2.8 mA/cm^2 at 20 °C, 3.4 mA/cm^2 at 30 °C, and 6 mA/cm^2 at 50 °C. As in the case of the anode performance, a higher performance was possible by increasing the temperature.

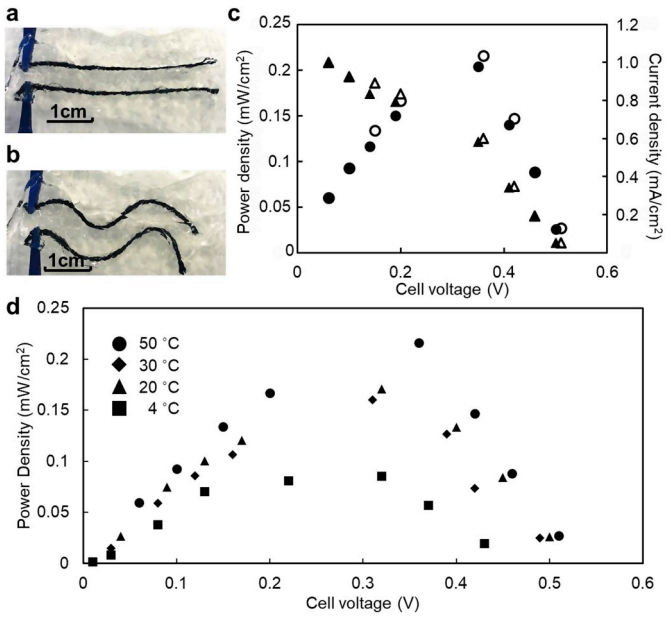

Fig. 4. a. Photograph of a biofuel cell operating on GDH- and BOD-based fibers. b. The deformation to S-shape. c. Performance of the fiber biofuel cell with and without the deformation at 50 °C. Hollow and solid circles denote the power densities of the undeformed and deformed cells, respectively. Hollow and solid triangles denote the current densities of the undeformed and deformed cells, respectively. d. Temperature dependency of the cell performance.

3.3. Performance of GDH/BOD fibered biofuel cells

A biofuel cell was constructed with the GDH-CNT composite fiber anode and the gas-diffusing BOD-CNT composite fiber cathode. Both fibers were placed on the surface of the hydrogel tank containing 200 mM glucose and 10 mM NAD^+ (Fig. 4a and b). The open-circuit voltage of the cell was 0.51 V, which reflected the difference between the potentials at which glucose oxidation and oxygen reduction started in cyclic voltammograms (−0.01 V in Figs. 2a and 0.5 V in Fig. 3a). The maximum power density was 216 μW/cm^2 at 0.36 V, and even when both fibers were deformed to an S-shape (Fig. 4b), we observed no significant loss of output power (Fig. 4c). Furthermore, we measured the cell performance at glucose concentrations, from 0.1 to 200 mM (Supporting Fig. 3) and temperatures from 4 °C to 50 °C (Fig. 4d). A decrease in the glucose concentration and in the temperature reduced the cell performance to 85 μW/cm^2 at 0.32 V under 4 °C and 200 mM glucose, or to 48 μW/cm^2 at 0.24 V under 50 °C and 0.1 mM glucose. Additionally, we confirmed the lifetime of the present cell on the cloth (Supporting Fig. 4). When we dropped a glucose solution at 1 mL/min, the cells retained the output above 90% at 72 h. However, when the cell was placed on the hydrogel tank, its initial performance (216 μW/cm^2) reduced dramatically to 62 μW/cm^2 in 2 h due to drying of the hydrogel tank. In fact, when we dropped a glucose solution, the reduced power output returned to its original value (204 μW/cm^2).

The “flexible and fiber-shaped” character of the enzyme electrode is an attractive advantage as a wearable power source because it allows sewing and tying of the fibers on textile cloth (Figs. 1b and 5). In Fig. 1b, our W-shaped BFC (single cell) woven on a cloth successfully powered the LED device with a charge pump (LED blinking at 1.33 Hz (Movie 1). Illuminating the LED without a charge pump requires the series connection to supply a voltage over 1.6 V, which is an operating voltage of the red LED. In Fig. 5, we demonstrated a series connection of four BFCs tied between the anode and cathode fibers on a cloth with batik-based ionic isolation. First, we created four-square units by applying melted wax to the fabric cloth with a paintbrush to confine the diffusion of electrolytes to the waxed square unit. We designed the

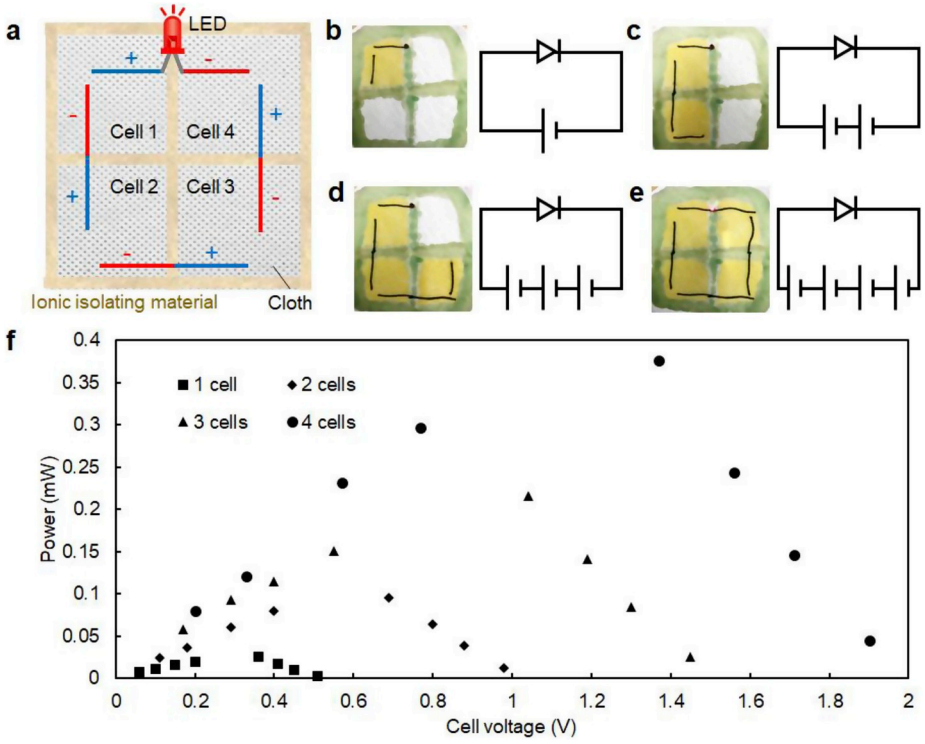

Fig. 5. a. Schematic of the four series-connected cells on the textile cloth. b–e. Pictures of an LED connected with (b) a single BFC and with series connecting (c) double, (d) triple, and (e) quadruple BFCs when we drop a solution, including a dye, 200 mM glucose, and 10 mM NAD^+. f. Performance of single, series-connected double, triple, and quadruple BFCs at 50 °C.

hydrophobic wax flame on the top surfaces of the cloth to avoid a short circuit between the cells on the cloth and through sweat electrolytes on the body when wearing the cloth (Supporting Fig. 5). After that, we sew both the anode and cathode fibers on the cloth inside each unit and then connected four cells in a series by tying both their anode and cathode fibers (Fig. 5a–e). An LED was connected to a BFC (Fig. 5b) or to a series of cells using double (Fig. 5c), triple (Fig. 5d), or quadruple BFCs (Fig. 5e). When we dropped a solution containing dye, 200 mM glucose, and 10 mM NAD^+ on the waxed cloth, the dye solution was confined to each unit. We observed a continuous LED light only when connected to the four series cells (Fig. 5e, Movie 2). We evaluated the performance of each cell to confirm these behaviors (Fig. 5f). The open-circuit voltage increased to 0.98 V for the double BFCs, 1.45 V for the triple BFCs, and 1.9 V for the quadruple BFCs, compared to 0.51 V obtained from a single BFC. The output voltage in quadruple BFCs exceeds the operating voltage of the red LED (over 1.6 V). These results indicate that we succeeded in establishing a series connection of four BFCs on a textile cloth, and its maximum power of 0.38 mW surpassed the 0.026 mW for a single BFC by a factor of 15.

4. Conclusions

We developed a wearable, high-powered biofuel cell using a glucose-oxidizing GDH-based anode and an O_2-diffusion BOD-based cathode on a textile cloth. To improve the performance of the anode and the cathode, we used two types of CNT layers: an acid-treated hydrophilic CNT layer for the mediator and the enzyme coating, and a PTFE-based hydrophobic CNT layer for adequate oxygen diffusion. Moreover, we optimized multiple CNT layer structures on carbon fibers in the bioanode and the biocathode. Using the optimized bioanode and biocathode, the maximum power density reached 216 μW/cm^2 at 0.36 V, even when the structure was deformed to an S-shape. To boost the output voltage of BFCs, we designed a series connection of four BFCs tied between their anode and cathode fibers with batik-based ionic isolation on the cloth. The open-circuit voltage was enhanced to 1.9 V for the quadruple BFCs as compared to 0.51 V for a BFC. We demonstrated illumination of a red LED connected with four BFCs in series. Such a flexible, soft power source highlights potential for combination in the future with wearable electronics.

Declaration of interests

The authors declare that they have no known competing financial interests or personal relationships that could have appeared to influence the work reported in this paper.

Acknowledgment

The research presented in this article was supported by the Tonen General Sekiyu Research Development Encouragement Foundation. Part of this work was conducted at the Nanotechnology Platform Kitakyushu User Facility.

Appendix A. Supplementary data

Supplementary data to this article can be found online at https://doi.org/10.1016/j.bios.2019.111471.

References

Akers, N.L., Moore, C.M., Minteer, S.D., 2005. Development of alcohol/O2 biofuel cells using salt-extracted tetrabutylammonium bromide/Nafion membranes to immobilize dehydrogenase enzymes. Electrochim. Acta 50 (12), 2521–2525.
Bandodkar, A.J., Jeerapan, I., You, J.-M., Nuñez-Flores, R., Wang, J., 2015. Highly stretchable fully-printed CNT-based electrochemical sensors and biofuel cells: combining intrinsic and design-induced stretchability. Nano Lett. 16 (1), 721–727.
Bandodkar, A.J., You, J.-M., Kim, N.-H., Gu, Y., Kumar, R., Mohan, A.V., Kurniawan, J., Imani, S., Nakagawa, T., Parish, B., 2017. Soft, stretchable, high power density electronic skin-based biofuel cells for scavenging energy from human sweat. Energy Environ. Sci. 10 (7), 1581–1589.
Bilgi, M., Sahin, E.M., Ayranci, E., 2018. Sensor and biosensor application of a new redox mediator: rosmarinic acid modified screen-printed carbon electrode for electrochemical determination of NADH and ethanol. J. Electroanal. Chem. 813, 67–74.
Carucci, C., Salis, A., Magner, E., 2017. Specific ion effects on the mediated oxidation of NADH. ChemElectroChem 4 (12), 3075–3080.
Dinh, T.H., Lee, S.C., Hou, C.Y., Won, K., 2016. Diaphorase-viologen conjugates as bioelectrocatalysts for NADH regeneration. J. Electrochem. Soc. 163 (6), H440–H444.
Falk, M., Andoralov, V., Blum, Z., Sotres, J., Suyatin, D.B., Ruzgas, T., Arnebrant, T.,

Shleev, S., 2012. Biofuel cell as a power source for electronic contact lenses. Biosens. Bioelectron. 37 (1), 38–45.
Göbel, G., Beltran, M.L., Mundhenk, J., Heinlein, T., Schneider, J., Lisdat, F., 2016. Operation of a carbon nanotube-based glucose/oxygen biofuel cell in human body liquids—performance factors and characteristics. Electrochim. Acta 218, 278–284.
Hammock, M.L., Chortos, A., Tee, B.C., Tok, J.B., Bao, Z., 2013. 25th anniversary article: the evolution of electronic skin (e-skin): a brief history, design considerations, and recent progress. Adv. Mater. 25 (42), 5997–6038.
Hanashi, T., Yamazaki, T., Tsugawa, W., Ikebukuro, K., Sode, K., 2011. BioRadioTransmitter: a Self-Powered Wireless Glucose-Sensing System. SAGE Publications.
Hattori, Y., Falgout, L., Lee, W., Jung, S.Y., Poon, E., Lee, J.W., Na, I., Geisler, A., Sadhwani, D., Zhang, Y., 2014. Multifunctional skin-like electronics for quantitative, clinical monitoring of cutaneous wound healing. Adv. Healthc. Mater. 3 (10), 1597–1607.
Ikeda, T., 2012. Bioelectrochemical studies based on enzyme-electrocatalysis. Electrochim. Acta 82, 158–164.
Jeerapan, I., Sempionatto, J.R., Pavinatto, A., You, J.-M., Wang, J., 2016. Stretchable biofuel cells as wearable textile-based self-powered sensors. J. Mater. Chem. 4 (47), 18342–18353.
Jia, W., Valdés-Ramírez, G., Bandodkar, A.J., Windmiller, J.R., Wang, J., 2013. Epidermal biofuel cells: energy harvesting from human perspiration. Angew. Chem. Int. Ed. 52 (28), 7233–7236.
Kassal, P., Kim, J., Kumar, R., de Araujo, W.R., Steinberg, I.M., Steinberg, M.D., Wang, J., 2015. Smart bandage with wireless connectivity for uric acid biosensing as an indicator of wound status. Electrochem. Commun. 56, 6–10.
Katz, E., 2015. Implantable biofuel cells operating in vivo—potential power sources for bioelectronic devices. Bioelectronic Medicine 2 (1), 1.
Katz, E., MacVittie, K., 2013. Implanted biofuel cells operating in vivo–methods, applications and perspectives–feature article. Energy Environ. Sci. 6 (10), 2791–2803.
Kwon, C.H., Lee, S.-H., Choi, Y.-B., Lee, J.A., Kim, S.H., Kim, H.-H., Spinks, G.M., Wallace, G.G., Lima, M.D., Kozlov, M.E., 2014. High-power biofuel cell textiles from woven biscrolled carbon nanotube yarns. Nat. Commun. 5, 3928.
Li, X., Zhou, H., Yu, P., Su, L., Ohsaka, T., Mao, L., 2008. A Miniature glucose/O2 biofuel cell with single-walled carbon nanotubes-modified carbon fiber microelectrodes as the substrate. Electrochem. Commun. 10 (6), 851–854.
Lv, J., Jeerapan, I., Tehrani, F., Yin, L., Silva-Lopez, C.A., Jang, J.-H., Joshuia, D., Shah, R., Liang, Y., Xie, L., 2018. Sweat-based wearable energy harvesting-storage hybrid textile devices. Energy Environ. Sci. 11 (12), 3431–3442.
Minteer, S.D., Liaw, B.Y., Cooney, M.J., 2007. Enzyme-based biofuel cells. Curr. Opin. Biotechnol. 18 (3), 228–234.
Miyake, T., Haneda, K., Nagai, N., Yatagawa, Y., Onami, H., Yoshino, S., Abe, T., Nishizawa, M., 2011a. Enzymatic biofuel cells designed for direct power generation from biofluids in living organisms. Energy Environ. Sci. 4 (12), 5008–5012.
Miyake, T., Haneda, K., Yoshino, S., Nishizawa, M., 2013. Flexible, layered biofuel cells. Biosens. Bioelectron. 40 (1), 45–49.
Miyake, T., Oike, M., Yoshino, S., Yatagawa, Y., Haneda, K., Kaji, H., Nishizawa, M., 2009. Biofuel cell anode: NAD+/glucose dehydrogenase-coimmobilized ketjenblack electrode. Chem. Phys. Lett. 480 (1–3), 123–126.
Miyake, T., Yoshino, S., Yamada, T., Hata, K., Nishizawa, M., 2011b. Self-regulating enzyme− nanotube ensemble films and their application as flexible electrodes for biofuel cells. J. Am. Chem. Soc. 133 (13), 5129–5134.
Murata, K., Akatsuka, W., Tsujimura, S., 2014. Bioelectrocatalytic oxidation of glucose on MgO-templated mesoporous carbon-modified electrode. Chem. Lett. 43 (6), 928–930.
Neto, S.A., Almeida, T., Belnap, D., Minteer, S., De Andrade, A., 2015. Enhanced reduced nicotinamide adenine dinucleotide electrocatalysis onto multi-walled carbon nanotubes-decorated gold nanoparticles and their use in hybrid biofuel cell. J. Power Sources 273, 1065–1072.
Nishizawa, M., 2019. Carbon Nanotube-Based Enzymatic Biofuel Cells. Nanocarbons for Energy Conversion: Supramolecular Approaches. Springer, pp. 351–370.
Ogawa, Y., Kato, K., Miyake, T., Nagamine, K., Ofuji, T., Yoshino, S., Nishizawa, M., 2015. Organic transdermal iontophoresis patch with built-in biofuel cell. Adv. Healthc. Mater. 4 (4), 506–510.
Oh, S.Y., Hong, S.Y., Jeong, Y.R., Yun, J., Park, H., Jin, S.W., Lee, G., Oh, J.H., Lee, H., Lee, S.-S., 2018. Skin-attachable, stretchable electrochemical sweat sensor for glucose and pH detection. ACS Appl. Mater. Interfaces 10 (16), 13729–13740.
Park, S.-I., Xiong, Y., Kim, R.-H., Elvikis, P., Meitl, M., Kim, D.-H., Wu, J., Yoon, J., Yu, C.-J., Liu, Z., Huang, Y., Hwang, K.-c., Ferreira, P., Li, X., Choquette, K., Rogers, J.A., 2009. Printed assemblies of inorganic light-emitting diodes for deformable and semitransparent displays. Science 325 (5943), 977–981.
Pillai, K.C., Shalini Devi, K.S., Senthil Kumar, A., Moon, I.-S., 2018. Selective and low potential electrocatalytic oxidation of NADH using a 2,2-diphenyl-1-picrylhydrazyl immobilized graphene oxide-modified glassy carbon electrode. J. Solid State Electrochem. 22 (11), 3393–3408.
Ramanavicius, A., Kausaite, A., Ramanaviciene, A., 2005. Biofuel cell based on direct bioelectrocatalysis. Biosens. Bioelectron. 20 (10), 1962–1967.
Sekitani, T., Nakajima, H., Maeda, H., Fukushima, T., Aida, T., Hata, K., Someya, T., 2009. Stretchable active-matrix organic light-emitting diode display using printable elastic conductors. Nat. Mater. 8 (6), 494.
Shitanda, I., Kato, S., Tsujimura, S., Hoshi, Y., Itagaki, M., 2017. Screen-printed, paper-based, array-type, origami biofuel cell. Chem. Lett. 46 (5), 726–728.
Shitanda, I., Nakafuji, H., Tsujimura, S., Hoshi, Y., Itagaki, M., 2015. Electrochemical impedance study of screen-printed branch structure porous carbon electrode using MgO-templated carbon and MgO particle and its application for bilirubin oxidase-immobilized biocathode. Electrochemistry 83 (5), 329–331.
Sim, H.J., Lee, D.Y., Kim, H., Choi, Y.-B., Kim, H.-H., Baughman, R.H., Kim, S.J., 2018. Stretchable fiber biofuel cell by rewrapping multiwalled carbon nanotube sheets. Nano Lett. 18 (8), 5272–5278.
Southcott, M., MacVittie, K., Halámek, J., Halámková, L., Jemison, W.D., Lobel, R., Katz, E., 2013. A pacemaker powered by an implantable biofuel cell operating under conditions mimicking the human blood circulatory system–battery not included. Phys. Chem. Chem. Phys. 15 (17), 6278–6283.
Sun, Q., Rabbani, P., Takeo, M., Lee, S.H., Lim, C.H., Noel, E.S., Taketo, M.M., Myung, P., Millar, S., Ito, M., 2018 Jul. Dissecting wnt signaling for melanocyte regulation during wound healing. J. Investig. Dermatol. 138 (7), 1591–1600. https://doi.org/10.1016/j.jid.2018.01.030. Epub 2018 Feb 8.
Tamaki, T., Ito, T., Yamaguchi, T., 2007. Immobilization of hydroquinone through a spacer to polymer grafted on carbon black for a high-surface-area biofuel cell electrode. J. Phys. Chem. B 111 (34), 10312–10319.
Togo, M., Morimoto, K., Abe, T., Kaji, H., Nishizawa, M., 2009. Microfluidic biofuel cells: series-connection with superhydrophobic air valves. In: TRANSDUCERS 2009-2009 International Solid-State Sensors, Actuators and Microsystems Conference. IEEE, pp. 2102–2105.
Weissenborn, P.K., Pugh, R.J., 1996. Surface tension of aqueous solutions of electrolytes: relationship with ion hydration, oxygen solubility, and bubble coalescence. J. Colloid Interface Sci. 184 (2), 550–563.
Willner, I., Yan, Y.M., Willner, B., Tel-Vered, R., 2009. Integrated enzyme-based biofuel cells–a review. Fuel Cells 9 (1), 7–24.
Yamada, T., Hayamizu, Y., Yamamoto, Y., Yomogida, Y., Izadi-Najafabadi, A., Futaba, D.N., Hata, K., 2011. A stretchable carbon nanotube strain sensor for human-motion detection. Nat. Nanotechnol. 6 (5), 296.
Yasuhira, K., Shibata, N., Mongami, G., Uedo, Y., Atsumi, Y., Kawashima, Y., Hibino, A., Tanaka, Y., Lee, Y.H., Kato, D., Takeo, M., Higuchi, Y., Negoro, S., 2010. X-ray crystallographic analysis of the 6-aminohexanoate cyclic dimer hydrolase: catalytic mechanism and evolution of an enzyme responsible for nylon-6 byproduct degradation. J. Biol. Chem. 285 (2), 1239–1248.